

A high transmittance color liquid crystal display mode with controllable color gamut and transparency

Byung-June Mun,¹ Wan Seok Kang,¹ Joun Ho Lee,² Hyun Chul Choi,² Byeong Koo Kim,² Bongsoon Kang,¹ Young Jin Lim,³ Seung Hee Lee,^{3,*} and Gi-Dong Lee^{1,4}

¹Department of Electronics Engineering, Dong-A University, Busan 604-714, South Korea

²LG Display Co., Ltd., Gumi, Gyungbuk 730-731, South Korea

³Applied Materials Institute for BIN Convergence, Department of BIN Fusion Technology, Chonbuk National University, Jeonju, Jeonbuk, 561-756, South Korea

⁴gdlee@dau.ac.kr

*lsh1@chonbuk.ac.kr

Abstract: In this paper, we propose a color transparent liquid crystal (LC) mode that can control the properties of the color gamut and transparency in a single panel. To achieve high transmittance in the transparent LC mode, a reactive mesogen (RM) with embedded color dichroic dyes was applied instead of a color filter. Basically, the LC mode applied a 3-terminal electrode structure to switch between the transparent LC mode and the conventional color LC mode. Depending on the direction of the applied voltage, we can operate both the color mode and the transparent mode in a single panel, and modulate the transparency and color purity of the cell through appropriate voltage control. In the experiments, we confirmed that the transmittance and the color gamut of the cell were 39.4% and 2% in the transparent LC mode and 14.9% and 34% in the color LC mode, respectively. Modulation of the color gamut and transparency between each LC mode are also demonstrated in the paper.

©2014 Optical Society of America

OCIS codes: (160.3710) Liquid crystals; (230.3720) Liquid-crystal devices.

References and links

1. B.-J. Mun, T. Y. Jin, G.-D. Lee, Y. J. Lim, and S. H. Lee, "Optical approach to improve the γ curve in a vertical-alignment liquid-crystal cell," *Opt. Lett.* **38**(5), 799–801 (2013).
2. Y. J. Lim, J. H. Kim, J. H. Her, K. H. Park, J. H. Lee, B. K. Kim, W.-S. Kang, G.-D. Lee, and S. H. Lee, "Viewing angle switching of liquid crystal display using fringe-field switching to control off-axis phase retardation," *J. Phys. D Appl. Phys.* **43**(8), 085501 (2010).
3. J.-H. Lee, J.-H. Son, S.-W. Choi, W.-R. Lee, K.-M. Kim, J. S. Yang, J. C. Kim, H. Choi, and G.-D. Lee, "Compensation for phase dispersion in horizontal-switching liquid crystal cell for improved viewing angle," *J. Phys. D Appl. Phys.* **39**(24), 5143–5148 (2006).
4. S. H. Ji and G.-D. Lee, "Advanced wide viewing angle technology in liquid crystal display modes," *Liq. Cryst.* **36**(6–7), 657–668 (2009).
5. Y. Kim, Y.-J. Lee, D.-H. Kim, J.-H. Baek, J.-H. Lee, B.-K. Kim, C.-J. Yu, and J.-H. Kim, "Fast response time of fringe-field switching liquid crystal mode devices with reactive mesogen in a planar alignment layer," *J. Phys. D Appl. Phys.* **46**(48), 485306 (2013).
6. W. S. Kang, J.-W. Moon, G.-D. Lee, S.-H. Lee, J.-H. Lee, B.-K. Kim, and H.-C. Choi, "Retardation free in-plane switching liquid crystal display with high speed and wide-view angle," *J. Opt. Soc. Korea* **15**(2), 161–167 (2011).
7. S. H. Lee, S. L. Lee, and H. Y. Kim, "Electro-optic characteristics and switching principle of a nematic liquid crystal cell controlled by fringe-field switching," *Appl. Phys. Lett.* **73**, 2881–2883 (1998).
8. A. Takeda, S. Kataoka, T. Sasaki, H. Chida, H. Tsuda, K. Ohmuro, T. Sasabayashi, Y. Koike, and K. Okamoto, "A super-high image quality multi-domain vertical alignment LCD by new rubbing-less technology," *Dig. Tech. Pap.* **29**(1), 1077–1088 (1998).
9. K. H. Kim, K. H. Lee, S. B. Park, J. K. Song, S. N. Kim, and J. H. Souk, "Domain divided vertical alignment mode with optimized fringe field effect," in *Proc. of the 18th International Display Research Conference/Asia Display* (Society for Information Display, Seoul, Korea, 1998), pp. 383–386.
10. J. F. Wager, "Transparent electronics-Display applications," *Dig. Tech. Pap.* **38**(1), 1824–1825 (2007).

11. C.-W. Kuo, C.-H. Lin, Y.-Y. Liao, Y.-H. Lai, C.-T. Chuang, C.-N. Yeh, J.-K. Lu, and N. Sugiura, "Blur-free transparent LCD with hybrid transparency," *Dig. Tech. Pap.* **44**(1), 70–73 (2013).
12. C.-H. Lin, W.-B. Lo, K.-H. Liu, C.-Y. Liu, J.-K. Lu, and N. Sugiura, "Novel transparent LCD with tunable transparency," *Dig. Tech. Pap.* **43**(1), 1159–1162 (2012).
13. E. Satoh, Y. Asaoka, K. Deguchi, I. Ihara, K. Minoura, S. Fujiwara, A. Miyata, Y. Itoh, Y. Iyama, M. Shibasaki, K. Kikuchi, and M. Kubo, "60-inch highly transparent see-through active matrix display without polarizers," *Dig. Tech. Pap.* **41**(1), 1192–1195 (2010).
14. B.-W. Lee, C. Park, S. Kim, T. Kim, Y. Yang, J. Oh, J. Choi, M. Hong, D. Sakong, K. Chung, S. Lee, and C. Kim, "TFT-LCD with RGBW color system," *Dig. Tech. Pap.* **34**(1), 1212–1215 (2003).
15. D. Cupelli, F. P. Nicoletta, S. Manfredi, M. Vivacqua, P. Formoso, G. De Filpo, and G. Chidichimo, "Self-adjusting smart windows based on polymer-dispersed liquid crystals," *Sol. Energy Mater. Sol. Cells* **93**(11), 2008–2012 (2009).
16. M. Macchione, G. De Filpo, F. P. Nicoletta, and G. Chidichimo, "Photochromic reverse mode polymer dispersed liquid crystal," *Liq. Cryst.* **32**(3), 315–319 (2005).
17. J. S. Gwag, K. Sohn, Y.-K. Kim, and J.-H. Kim, "Electro-optical characteristics of a chiral hybrid in-plane switching liquid crystal mode for high brightness," *Opt. Express* **16**(16), 12220–12226 (2008).
18. M. Mitov and N. Dessaud, "Cholesteric liquid crystalline materials reflecting more than 50% of unpolarized incident light intensity," *Liq. Cryst.* **34**, 183–193 (2007).
19. J. Yeon, J.-H. Lee, J.-B. Yoon, J. Park, and D. Kang, "A new reflective-type transparent display using cholesteric liquid crystal," *Dig. Tech. Pap.* **41**(1), 838–841 (2010).
20. T. Uchida, S. Yamamoto, and Y. Shibata, "A full-color matrix liquid-crystal display with color layers on the electrodes," *IEEE Trans. Electron. Dev.* **30**(5), 503–507 (1983).
21. C. P. Chen, K.-H. Kim, T.-H. Yoon, and J. C. Kim, "A viewing angle switching panel using guest-host liquid crystal," *Jpn. J. Appl. Phys.* **48**(6), 062401 (2009).
22. T. Sonehara, "Photo-addressed liquid crystal SLM with twisted nematic ECB (TN-ECB) mode," *Jpn. J. Appl. Phys.* **29**(7), L1231–L1234 (1990).
23. Y. Itoh, H. Seki, T. Uchida, and Y. Masuda, "A double-layer electrically controlled birefringence liquid-crystal display with a wide-viewing-angle cone," *Jpn. J. Appl. Phys.* **30**(7B), L1296–L1299 (1991).
24. S. G. Kim, S. M. Kim, Y. S. Kim, H. K. Lee, S. H. Lee, G.-D. Lee, J.-J. Lyu, and K. H. Kim, "Stabilization of the liquid crystal director in the patterned vertical alignment mode through formation of pretilt angle by reactive mesogen," *Appl. Phys. Lett.* **90**(26), 261910 (2007).
25. S. M. Kim, I. Y. Cho, W. I. Kim, K.-U. Jeong, S. H. Lee, G.-D. Lee, J. Son, J.-J. Lyu, and K. H. Kim, "Surface-modification on vertical alignment layer using UV-curable reactive mesogens," *Jpn. J. Appl. Phys.* **48**(3), 032405 (2009).
26. M. Schadt and W. Helfrich, "Voltage-dependent optical activity of a twisted nematic liquid crystal," *Appl. Phys. Lett.* **18**(4), 127–128 (1971).
27. S.-T. Wu, U. Efron, and L. D. Hess, "Optical rotatory power of 90° twisted nematic liquid crystal," *Appl. Phys. Lett.* **44**(9), 842–844 (1984).
28. P. Yeh and C. Gu, *Optics of Liquid Crystal Displays* (Wiley Interscience, 1999), Chap. 4.3.1, p. 123.
29. I. H. Yu, I. S. Song, J. Y. Lee, and S. H. Lee, "Intensifying the density of a horizontal electric field to improve light efficiency in a fringe-field switching liquid crystal display," *J. Phys. D Appl. Phys.* **39**(11), 2367–2372 (2006).

1. Introduction

Liquid crystal display (LCD) technologies have been developed to provide better electro-optical characteristics such as a wide viewing angle, fast response time, and high contrast ratio [1–9]. In spite of superior optical performances, studies on advanced LCD technologies are still required to realize more convenient and interactive display performance. Recently, one of the most important issues of the next-generation LCDs appears to concern transparent-display technology [10–13]. Especially, transparent displays can simultaneously show both conventional color images and background images behind the panel by using transparent optical devices. Moreover, this optical performance can produce a new visual experience to attract the viewer's attention, and can be applied not only to displays, but also to many different fields, including advertisements, transportation, medical, military, and interior design applications.

In order to enable an excellent transparent-display performance, the light efficiency of the panel must be improved to obtain high transparency characteristics. However, the conventional LCD mode normally exhibits very low transmittance of ~5% due to several of its optical elements such as its thin-film transistor (TFT), electrodes, color filter, and polarizers [11, 12, 14]. Especially, color filters and polarizers lead to a decrease in transmittance of more than 80%. To overcome this loss in light transmittance, several transparent LCD modes such as the polymer-dispersed LC (PDLC) mode [15, 16], the

cholesteric LC (Ch-LC) mode [17–19], and guest-host (G-H) mode [20, 21] have been developed. These modes, which are representative of polarizer-free modes, can exhibit high transmittance by using the optical property of the light instead of the polarizer. In these modes, however, high transmittance can deteriorate the color gamut for vivid image quality due to the trade-off relation between the transmittance and color purity in the transparent mode. Therefore, the development of a novel LC mode with high transmittance and good color purity has become an important research goal.

In this paper, we proposed a LC mode that can switch between the color LC mode and the transparent LC mode by using a 3-terminal electrode structure. Basically, we used a black dye-doped LC mixture for achieving a superior dark state in the transparent mode. In addition, we established a reactive mesogen (RM) with embedded red (*R*), green (*G*), and blue (*B*) color dichroic dyes on the top substrate instead of using pigment-dispersed color filter to achieve a full-color state in the transparent cell. By controlling the voltage direction through the 3-terminal electrode in the cell, we could switch the optical properties of the color mode and the transparent mode. In addition, we could also modulate the optical and color properties between the color mode and the transparent mode by applying the appropriate voltage.

2. Cell structure and the electro-optical principle of the proposed transparent LC cell

Figure 1 shows the proposed cell structure for the transparent and color display mode. To switch between the conventional color LC mode and transparent LC mode, the 3-terminal electrode structure, which consists of two common electrodes and a patterned electrode, is used. The top substrate had a basic electrode layer for each color dye area. On the bottom substrate, the upper electrode layer was used as the patterned electrode with an electrode width of 4 μm and interval 4 μm between the patterned electrodes, and lower electrode layer had common electrode. In this cell, RM with embedded color dichroic dyes, which has an alignment direction to the *x*-axis, is established on the top substrate to realize the color LC mode with high transmittance in the proposed transparent LC cell.

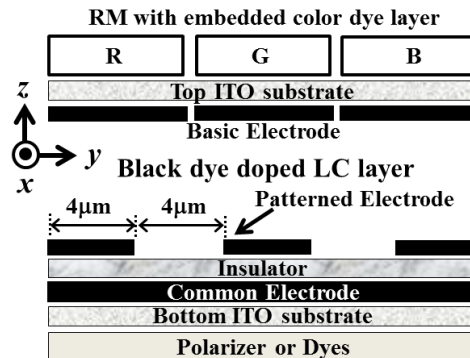


Fig. 1. Schematic diagram of the cell and electrode structure for the transparent LC mode.

Figure 2 illustrates the three modes in the transparent cell. In the initial dark mode, we used the electrically controlled birefringence (ECB) mode [22, 23] that is rubbed antiparallel to the *x*-direction, as shown in Fig. 2 (a). In this state, incident polarized light passes through the transparent LC cell without any change in the polarization. Therefore, all of the light wavelengths are strongly absorbed by the black and color dyes. In the conventional color LC mode and transparent LC mode, a vertical alignment (VA) mode [24, 25] and twisted nematic (TN) mode [26, 27] were respectively used by applying the voltage to the 3-terminal electrode. In the VA mode which is homeotropic state in Fig. 2 (b), the incident light is not affected in the black dye layer because of the orthogonality between the two optical axes of the polarized light and black dyes. However, after passing through the color dye layer, the light contains the specific color wavelengths from the dichroic color dyes; thus, the color LC

mode can be realized in a cell. On the other hand, the transparent mode applies a fringe electric field between the two electrodes on the bottom substrate. In this case, the LCs and black dyes on the bottom surface are reoriented in the y -direction, and the polarization axis of the incident light in the black dye layer is also rotated in the y -direction due to the wave-guiding effect in the o -mode, especially when patterned electrode is finely patterned [28,29]. Finally, the light passing through the proposed transparent LC cell is optically transmitted without the absorption of wavelengths, as shown in Fig. 2(c). Two modes are controlled by appropriately applying the voltage to 3-terminal electrode so that the color gamut and transparency can be modulated in a single pixel. The electro-optic performance of the proposed device will be better as the dichroic ratio of embedded dye is higher.

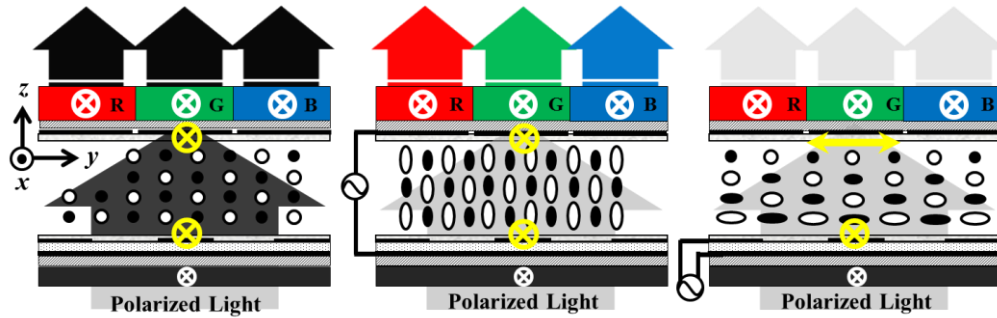


Fig. 2. Electro-optical principle of the three LC modes in the proposed transparent LC cell: (a) an initial dark mode, (b) a color LC mode and (c) a transparent LC mode.

3. Experiments and discussions

Figure 3 shows the schematic of the fabrication process. We prepared the two substrates with the 3-terminal electrode structure in Fig. 3(a). A polyamic acid (PA) type of alignment layer (AL16301K, JSR Micro Korea) was spin-coated on two prepared substrates to align the cell layers. Next, the PA was pre-baked at 100°C for 10 min, followed by hard baking at 230°C for 2 hours for the polymerization to be completed. In case of the top substrate, the coating was performed on both sides due to the alignment of the black and color dye layers as shown in Fig. 3(b). In this case, one side of PA layer can be destroyed if spin-coating for both sides of a substrate was performed. Thus, we performed the prebaking process for top substrate during the long time (>10 min) than bottom substrate to obtain the partial-imidization state of the PA layer. From the simple experiment, we could achieve that the alignment layer on both side of top substrate was successfully established without any destruction of both alignment layers. The surface was rubbed antiparallel to the x -axis, as mentioned above. To establish the color dye layer, we embedded the RM (SIR-W057C, Osaka Organic Chemical, Japan), and the R , G , and B color dichroic dyes. The color property of each color layer is obviously dependent on the solubility of the color dyes to the RM material, which means high solubility of the dye material makes high color purity and broad color gamut. In this experiment, the mixture ratio was 2.47wt% of red dyes, 4wt% of green dyes, and 0.5wt% of blue dyes, respectively. As shown in Fig. 3(c), the blue dye mixture was initially spin-coated onto the upper surface of the top substrate. Then, the mixture was exposed to the UV light source of 150mW/cm² for 15 sec through a photo-mask in Fig. 3(d), followed by pre-baking at 60 °C for 5 min. Next, the unexposed area was washed by using the developer solution (Osaka Organic Chemical, Japan) in Fig. 3(e) so that the blue dye area could be patterned. The green and red dyes were then added using the same process with UV exposure conditions of ~100mW/cm², and ~30mW/cm² for 15 sec, respectively. However, stacked three-color dyes can be contaminated because of the strong chemical reaction that occurs between the dyes. To solve this simple problem, the NOA68 (Norland Products Inc., USA) was covered on the fabricated dye area after attaching the mask tape between the patterned areas in Fig. 3(f) and cured with UV light, as shown in Fig. 3(g). To coating with the other color dyes, the mask

tapes were then removed in Fig. 3(h). As a result, we could fabricate the three-color dye layer as shown in Fig. 3(i). We finally assembled the two substrates and maintained the cell thickness by using a spacer. In order to make an excellent dark state of the cell, we found maximum soluble state of the black dye material to the LC material. In this experiment, we formed black dyes by mixing the *R*, *G* and *B* color dye. The optimized black dye-doped LC (MLC-7037, $\Delta\epsilon = 5$, and $\Delta n = 0.1144$, Merck) mixture with dye doping amount of 2.7 wt% was injected into two substrates as shown in Fig. 3(j).

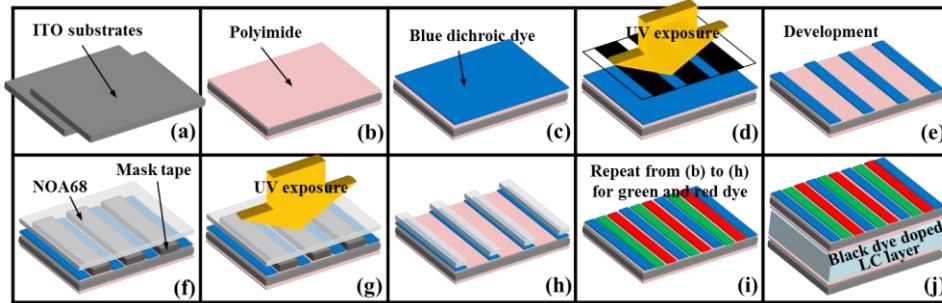


Fig. 3. Schematic diagram for the process steps of the transparent LC cell fabrication.

The optical properties in color mode, transparent mode and intermediate color mode can be simply calculated by calculating polarization state in front of the color dye layer. In calculation, we used the commercial LC software TechWiz LCD provided by the Sanayi System Co. in Korea. Figure 4 shows the calculated optical transmittance of the *R*, *G*, and *B* color dye layer in the proposed optical structure at 11 μm cell gap. In this figure, intermediate color state can be controlled by applying the voltage to the 3-terminal electrode.

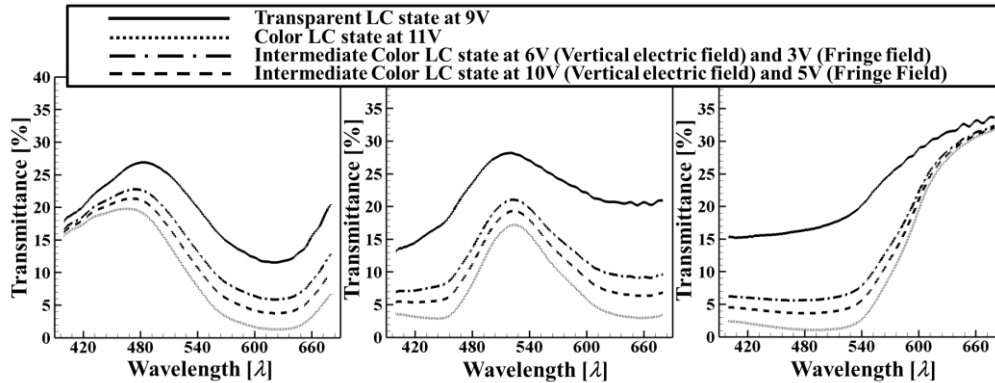


Fig. 4. The calculated optical transmittance of the proposed transparent LC mode in color mode, transparent mode and intermediate color mode: (a) blue area, (b) green area and (c) red area.

From this calculated results, we can also calculate the color property of the proposed optical structure. Figure 5 shows the calculated color property of the LC cell in color mode, transparent mode and intermediate color mode. From this, we can confirm that the color property can be controlled between the color gamut in color mode and transparent mode by appropriating voltage.

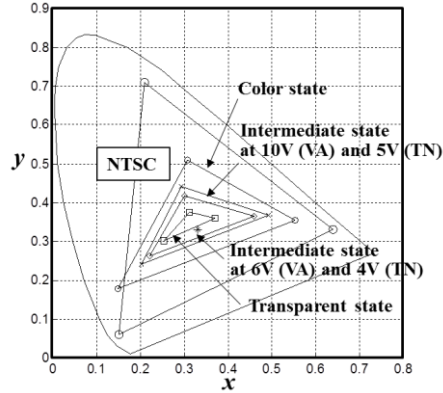


Fig. 5. The calculated color properties of the proposed transparent LC cell in color mode, transparent mode and intermediate color mode.

Figure 6 shows the microscopic image for the *R*, *G*, and *B* areas of the fabricated color-dye layer. In the parallel state between the polarization axis and the absorption axis of dyes as shown in Fig. 6(a), we could confirm the good color purity of each dye. On the other hand, all of the light wavelengths in the perpendicular state pass through the color layer except small absorption, as shown in Fig. 6(b). Therefore, we expected that the conventional LC mode and transparent LC mode could be simultaneously operational in a single panel.

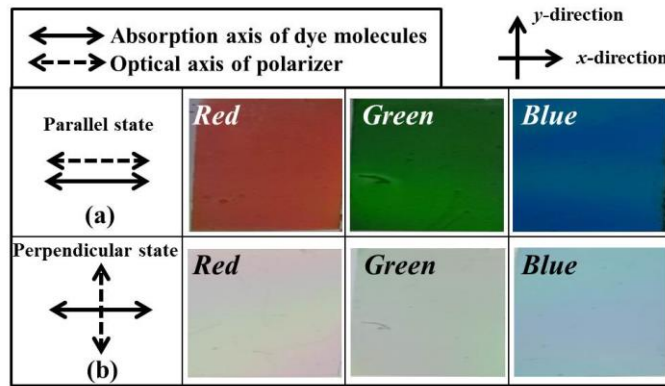


Fig. 6. Microscopic image for the *R*, *G* and *B* areas of the fabricated color dye layer (a) in a parallel state and (b) in a perpendicular state between the polarization axis and the absorption axis of the color dyes.

To verify the electro-optical performance of the proposed mode, we measured the transmittance of the cell by using a spectrometer (SPTR-100, Sesim LCD Co.). In the experiment, we applied a $1\text{V}/\mu\text{m}$ electric-field strength to the color LC mode and 9V to the transparent LC mode of the cell. Figure 7 shows the transmittance graph of the *R* (square), *G* (diamond), and *B* (circle) areas in the three modes as a function of the cell thickness. In the initial dark mode, the optimized black dye-doped LC mixture could induce a superior dark level; especially, the transmittance at the $32\mu\text{m}$ cell gap was minimized due to the high absorbance of the light in the high cell gap. Moreover, the transmittance of the color LC mode and transparent LC mode was highly enhanced by the presence of two dye layers. As a calculation result of the total transmittance of the cell, we achieved high transmittance of more than 15% in the color LC mode and 40% in the transparent LC mode, respectively.

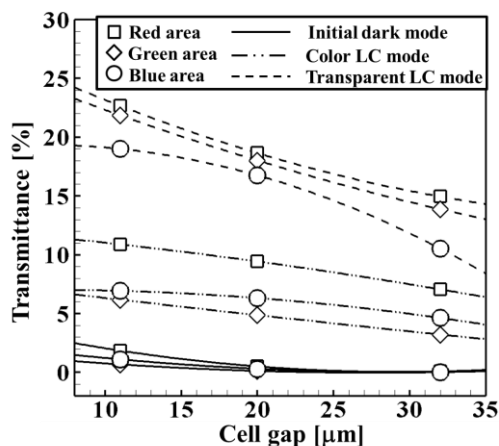


Fig. 7. Measured transmittance graph of the *R*, *G* and *B* areas in three modes as a function of the cell thickness.

Figures 8(a) and 8(b) represent the measured chromaticity diagrams (CIE 1931) of the *R*, *G*, and *B* areas in the color and transparent LC modes. The measured color gamut compared well with the National Television Standard Committee (NTSC) color gamut, which is the standard ratio for the triangular area of the color gamut. In the transparent LC mode, we confirmed that each color point was closely located around the white point with the symbol (*), as shown in Fig. 8(a). The color gamut area was approximately 2% when compared with the NTSC standard. In the color LC mode, however, the color gamut was largely widened by more than 30% for each cell gap through the optimized solubility of the color dyes, as can be seen in Fig. 8(b). From these experimental results, we confirmed that the proposed transparent cell can modulate the color gamut between the color LC mode and transparent LC mode so that we realized controllable transparency in a single panel.

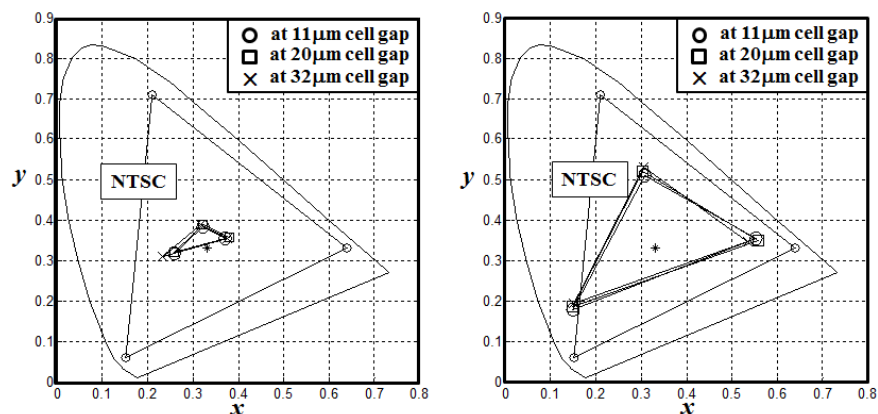


Fig. 8. Chromaticity diagrams (CIE 1931) of the proposed transparent LC cell (a) in the transparent LC mode and (b) in the color LC mode.

4. Conclusions

In summary, we proposed a switchable LC mode between a transparent LC mode and a color LC mode for transparent LCD applications. By using the RM mixed-color dichroic dyes on a substrate instead of a color filter, we achieved superior color purity and high transmittance in the cell. Furthermore, a black dye-doped LC mixture induced a good dark level so that the LC cell could show a high contrast ratio in the transparent mode. Through the experiments, we confirmed that the color LC mode and transparent LC mode are switched according to the

direction of the applied electric field to the 3-terminal electrode. Therefore, the color purity between the color LC mode and transparent LC mode could be modulated in the proposed LC cell. As results, the proposed LC mode realized both high transmittance and controllable transparency in a single panel. Obviously, the chemical and optical property of the color dye material can be one of most important factor that decides the electro-optical characteristics of the LC cell. Therefore, application of the good dye material to the proposed transparent LC mode will make the electro-optical characteristics of the LC mode excellent.

Acknowledgments

This work was supported by LG Display and the Basic Science Research Program through the National Research Foundation of Korea funded by the Ministry of Education, Science, and Technology.